Principal Line-Based Alignment Refinement for Palmprint Recognition

Wei Li, Bob Zhang, *Member, IEEE*, Lei Zhang, *Member, IEEE*, and Jingqi Yan

***Abstract*—Image alignment is an important step in various biometric authentication applications such as palmprint recognition. Most of the existing palmprint alignment methods make use of some key points between fingers or in palm boundary to establish the local coordinate system for region of interest (ROI) extraction. The ROI is consequently used for feature extraction and matching. Such alignment methods usually yield a coarse alignment of the palmprint images, while many missed and false matches are actually caused by inaccurate image alignments. To improve the palmprint verification accuracy, in this paper, we present an efficient palmprint alignment refinement method. After extracting the principal lines from the palmprint image, we apply the iterative closest point method to them to estimate the translation and rotation parameters between two images. The estimated parameters are then used to refine the alignment of palmprint feature maps for a more accurate palmprint matching. The experimental results show that the proposed method greatly improves the palmprint recognition accuracy and it works in real time.**

***Index Terms*—Biometrics, image alignment, line extraction, palmprint recognition.**

I. Introduction

AUTOMATIC personal authentication using biometric information plays an important role in applications of public security, access control, forensic, banking, etc. A variety of biometric authentication techniques have been developed in the past decades. Generally speaking, the biometric characteristics can be divided into two categories: physiological traits, such as fingerprint, face, iris, palmprint, hand shape, etc., and behavioral traits, such as signature, voice, gait, etc. Every field has been deeply researched. For example, fast Haar transform-based [25], L1-norm-based [26], and Gabor-based [27] methods had been proposed for face recognition. As a physiological biometric characteristic, palmprint was first used for personal recognition about ten years ago [1], and it has been widely studied due to its merits such as distinctiveness, cost-effectiveness, user friendliness, high accuracy, and so on. Various palmprint recognition systems have been set up and many palmprint recognition algorithms have been proposed [1]–[13].

According to the resolution of palmprint images, the palmprint recognition technique can be classified as high-resolution (at least 400 dpi) and low-resolution (less than 150 dpi) approaches. High-resolution palmprint recognition is basically used in law enforcement applications [5], while low-resolution approach can be widely used in civil and commercial applications [3]. Most of the current researches focus on low-resolution palmprint recognition, which has two main branches. The first one is coding-based methods, such as PalmCode [3], competitive code (CompCode) [4], Ordinal Code (OrdCode) [6], Fusion Code [8], robust line orientation code (RLOC) [13], etc. These methods use a group of filters to enhance and extract the phase or directional features of the palmprint and then encode these features into binary codes for fast matching. The other branch is line-based methods. These methods use some line or edge detectors to explicitly extract the line information from the palmprint and then use them for matching. The representative methods include derivative of Gaussian-based line extraction method [9], modified finite Radon transform (MFRAT)-based line extraction method [12], etc.

In general, the main steps in low-resolution palmprint recognition include data collection, region of interest (ROI) extraction, feature extraction, matching, and decision making. ROI extraction is a crucial step and it greatly affects the final recognition results. Most of the existing methods extract ROI according to some key points between fingers or in palm boundary, or some external factors [3], [7], [11].

Fig. 1(a) illustrates a two-key-points-based ROI extraction method used in [3]. It first searches for the two key points in the two gaps: one is between the forefinger and the middle finger, and the other one is between the ring finger and the little finger; then, a coordinate system can be set up according to the two key points; finally, the ROI can be extracted as a constant square under this coordinate system. Fig. 1(b) shows a three-key-points-based ROI extraction method proposed by Connie *et al.* [7]. This method first applied the salient-point detection algorithm [15] to obtain three key points, i.e., v_1, v_2, and v_3, then, connected v_2 and v_1, v_2, and v_3 as two reference lines, and after that, extended the two reference lines to intersect with the boundary of the hand which lead to find the two midpoints, m_1 and m_2; finally, based on the principal of

Manuscript received September 8, 2011; revised February 4, 2012; accepted March 26, 2012. Date of publication May 21, 2012; date of current version December 17, 2012. This work was supported in part by Guangdong Innovation Research Team Fund for low-cost healthcare technologies and by China National 973 Project (2011CB302203). This paper was recommended by Associate Editor X. Li.

W. Li is with the Shenzhen Institutes of Advanced Technology, Chinese Academy of Sciences, Shenzhen, China, and also with Huawei Technologies Co., Ltd., Shenzhen, China (e-mail: liweistorm@126.com).

B. Zhang is with the Department of Electrical and Computer Engineering, University of Waterloo, Waterloo, ON N2L 3P1, Canada (e-mail: yibo@pami.uwaterloo.ca).

L. Zhang is with the Department of Computing, Biometric Research Center, The Hong Kong Polytechnic University, Kowloon, Hong Kong (e-mail: cslzhang@comp.polyu.edu.hk).

J. Yan is with the Institute of Image Processing and Pattern Recognition, Shanghai Jiao Tong University, Shanghai 200240, China (e-mail: jqyan@sjtu.edu.cn).

Color versions of one or more of the figures in this paper are available online at http://ieeexplore.ieee.org.

Digital Object Identifier 10.1109/TSMCC.2012.2195653

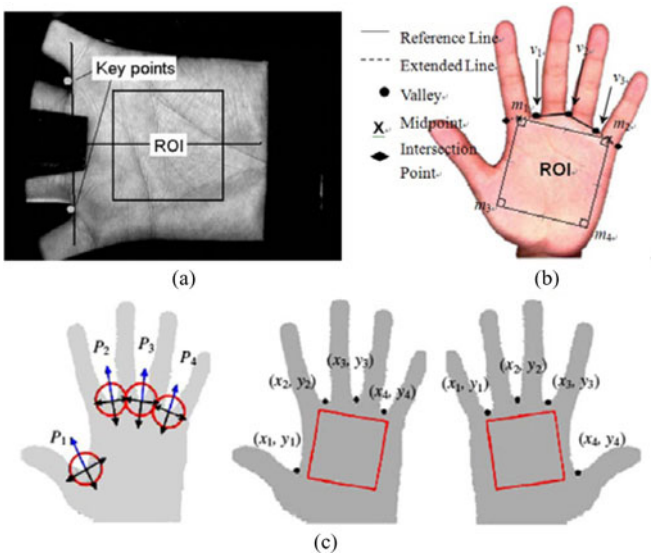

Fig. 1. Three typical ROI extraction methods [3], [7], [11].

geometrical square where all the four edges having equal length, the ROI is obtained. Fig. 1(c) describes a four-key-points-based ROI extraction method proposed by Michael *et al.* [11]. They first proposed a competitive valley detection algorithm to find the four key points, i.e., P_1, P_2, P_3, and P_4, and gave a rule to determine the right and left hands, and dealt with the right and left hands, respectively. The ideas of these methods are similar. All of them locate some key points from the gaps between fingers which decide the position of ROI. However, the palm is not a rigid object and there is no sharp corner on it, which makes the accurate localization of key points very hard. Thus, those ROI extraction methods can be used for a coarse alignment of palmprint images, and there are still some translation and rotation variations after ROI extraction. Although shifting the matching template [4] or using the "one to many" matching strategy [13] can deal with the small translation and rotation, they are time consuming and cannot truly solve the rotation effects.

Most of the existing palmprint recognition methods assume that the palmprint images have been well aligned before performing feature extraction and matching. Therefore, they are much affected by the residual translation and rotation variations after the alignment process like what is shown in Fig. 1. The coding-based palmprint recognition methods extract the local features from ROI for matching, while line-based methods exploit the global structural features in similarity measuring. These two types of methods use different techniques in feature extraction and matching. In general, the local features are more powerful to distinguish the palmprints, and hence, the coding-based methods often have higher accuracy than line-based methods. However, the line features can reflect the global transformation between palmprint images. This inspires us to develop a new palmprint recognition strategy: using the line features to refine the image alignment, and then using the local features for palmprint matching.

To more effectively and accurately correct the translation and rotation variations between palmprint images, we propose a new palmprint alignment strategy by adapting the iterative closest point (ICP) method to the palmprint principal lines, which are the most significant and stable features on palmprint. This idea has been mentioned in our conference paper [22]. In this paper, much more experiments and analyses have been done, such as the analysis on the robustness of principal line extraction, the comparison with template-shifting-based matching method, the proposition of an efficient matching scheme, and so on. The ICP algorithm is a classical method that was originally proposed for 3-D shape registration [14], [19], and it is also well suited to align 2-D curves. In the proposed algorithm, the principal lines are first extracted from ROI. Then, the ICP algorithm is used to estimate the translation and rotation parameters between two ROIs according to the extracted principal lines. With the estimated parameters, the palmprint ROIs can be better aligned to reduce the translation and rotation variations. The refined alignment of ROIs can bring great benefit in the consequent palmprint recognition.

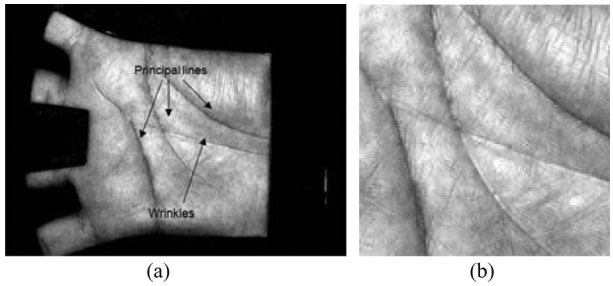

Fig. 2. (a) Principal lines and wrinkles on palmprint. (b) ROI image of (a).

The rest of this paper is organized as follows. Section II introduces and analyzes the principal line extraction method used in this paper. Section III describes the proposed ICP alignment method for palmprint recognition. Section IV presents the experimental results, and Section V gives the conclusion.

II. Principal Line Extraction

Fig. 2(a) shows a low-resolution (about 75 dpi) palmprint image. As can be seen, principal lines are the most stable and important features in low-resolution palmprint images. Fig. 2(b) shows the extracted ROI of Fig. 2(a) by using the method in [3] (see Fig. 1(a) for illustration). Although the ROI extraction reduces much the translation and rotation of palmprint images, there is still much room to further improve the palmprint alignment for higher recognition accuracy. In this paper, we propose to extract the principal lines and apply ICP to them for palmprint alignment refinement.

A. Principal Line Extraction Procedures

General line or edge detection methods, such as Canny edge detector [16] and Sobel edge detector [17], will extract too many trivial line features from the palmprint. This will introduce much difficulty to the following ICP correction step. Plain and clear line features will make the ICP process converge correctly and rapidly. In this paper, we adopt Huang's method [12], which is based on the Radon transform [18], for principal line extraction,

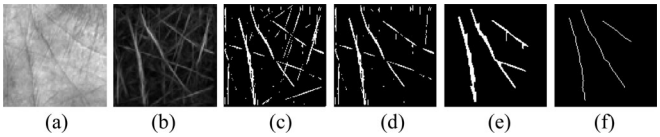

Fig. 3. Extraction of principal lines. (a) Original ROI. (b) Energy image. (c) Binary image of (b) after thresholding. (d) Image after minor lines removal of (c). (e) Line map after morphological operation on (d). (f) Finally thinned principal lines.

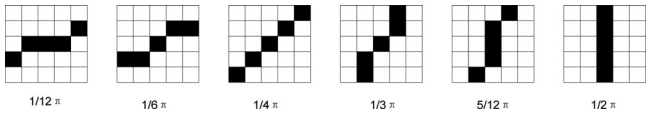

Fig. 4. Directional line structure templates used in the dilation operation.

and then use a series of postprocessing operations to enhance the line extraction results.

An MFRAT was proposed in [12] for principal line extraction:

$$r[L_k] = L_k * (g * H - H), \quad k = 1, 2, \ldots, N \tag{1}$$

where H represents an $m \times n$ image, g is a Gaussian filter, L_k denotes square template of line structure, and N is the total number of templates. An energy image E and a direction image D are then calculated as follows:

$$E(i,j) = \max(|r_{i,j}[L_k]|), i = 1, 2, \ldots, m, \ j = 1, 2, \ldots, n \tag{2}$$

$$D(i,j) = \arg\max_k(|r_{i,j}[L_k]|), \quad i = 1, 2, \ldots, m, \ j = 1, 2, \ldots, n \tag{3}$$

where $|\cdot|$ denotes the absolute value. The principal lines are extracted based on E and D. More details can be found in [12]. With images E and D, and by using some postprocessing steps to remove small wrinkles and trivial structures, the finally thinned principal lines can be well obtained. Fig. 3 illustrates the line extraction process by using an example.

Fig. 3(a) shows an original ROI. Fig. 3(b) shows the associated energy image E calculated by (2). Fig. 3(c) shows the binarized image of (b) after thresholding. In this step, we preserve the top 10% points with the highest energy in E. Fig. 3(d) is obtained from (c) by removing the minor directional lines. In general, the direction of principal lines in palmprint images is either within $[0, \pi/2]$ or within $[\pi/2, \pi]$. We partition the points in (c) into two classes according to whether their directions are greater or less than $\pi/2$. Then, the energy of each of the two classes is calculated as the summation of the energy of all points in that class. If the energy of class $[0, \pi/2]$ is lower, then the minor direction of the map in (c) is defined as $[0, \pi/2]$ or *vice versa*. Fig. 3(e) shows the line map after some morphological operations on (d), including *Dilation* operations according to the direction image D to connect the broken lines (Fig. 4 shows several masks of different directions for dilation), *Close* operations by a 3×3 square mask to remove small holes on the lines, and *Open* operations by a circle mask to remove short lines and small blocks. Fig. 3(f) illustrates the final line extraction result by thinning (e) and removing branches.

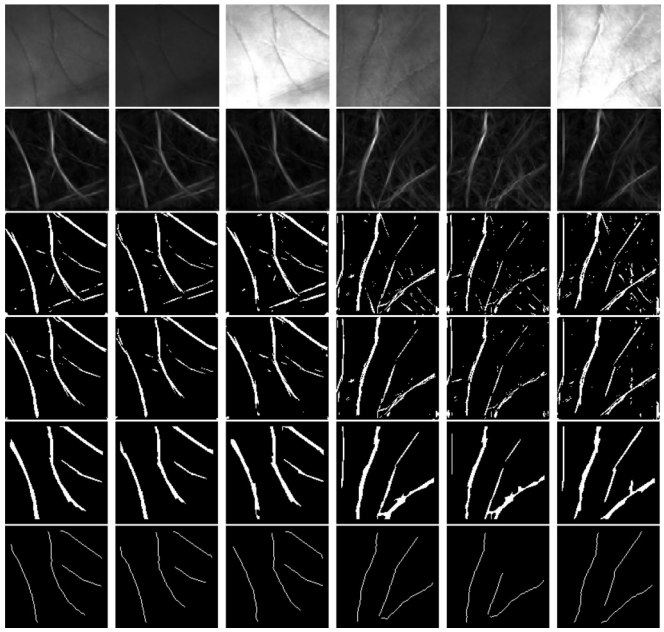

Fig. 5. Tests of principal line extraction on samples that have illumination variations and broken lines. First row: ROI images collected under different illumination conditions from two palms. Second row: energy images. Third row: binarized images. Fourth row: images after minor line removal. Fifth row: line maps after morphological operations. Sixth row: the final thinned principal lines.

B. Analysis on the Robustness of Principal Line Extraction

Considering that the results of principal line extraction will be crucial to the subsequent palmprint alignment refinement and recognition steps, it is necessary to discuss the robustness of principal line extraction under various conditions. Therefore, in the following, we make some tests and analyses of the principal line extraction procedures.

1) Dealing With Illumination Variations and Broken Lines: Fig. 5 verifies the principal line extraction on images which have illumination variations and broken lines. From Fig. 5, we can see that the used principal line extraction method is affected little by illumination variation. This is because the energy image defined in (2) is local contrast invariant. In Fig. 5, the first row shows several ROI images collected under different illumination conditions from two palms; the second row shows their energy images; the third row shows the binarized images; the fourth row shows the images after removing the minor lines; the fifth row gives the line maps after morphological operation; and the sixth row is the finally thinned principal lines. The morphological operation process can connect broken lines as shown in the fourth column of Fig. 5. However, if the line gap is greater than 5 pixels, this process will not connect the broken lines, as shown in some images in the fifth column of Fig. 5. Fortunately, ICP algorithm is robust to align two point sets which have partial overlap. According to our experience, the transformation parameters between the two ROIs can be well estimated by applying ICP to the principal lines extracted by the proposed procedures.

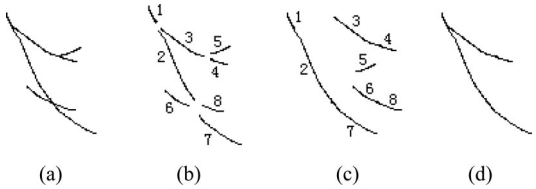

Fig. 6. Small line branch removal. (a) Original line. (b) Line segments of (a) by locating the intersections. (c) Connected branches according to the direction at intersections. (d) Remaining lines after small branch removal.

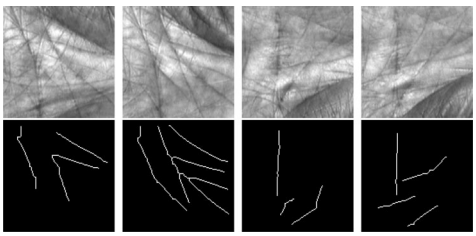

Fig. 7. Example palmprint images which are hard to extract stable principal lines.

TABLE I
ALGORITHM OF PRINCIPAL LINE-BASED ICP ALIGNMENT

Input	Two principal line point sets: $P=\{\vec{p}_i\}$ and $Q=\{\vec{q}_j\}$, $i=1,2,\cdots,N$, $j=1,2,\cdots,M$, suppose $N\le M$.
Output	Translation and rotation parameters T and R.
Initialization	$T=\begin{bmatrix}0\\0\end{bmatrix}$ and $R=\begin{bmatrix}1&0\\0&1\end{bmatrix}$.
Loop	1) For every point $\vec{p}_i$ in P, find the closest point $\vec{q}_j$ $j\in\{1,2,\cdots,M\}$ in Q to get the corresponding point pair $\{\vec{p}_i,\vec{q}_i'\}$, $i=1,2,\cdots,N$, where $\vec{q}_i'=\vec{q}_j$. 2) Calculate the mean distance of corresponding point pairs: $\bar{E}_{PQ}=\frac{1}{N}\sum_{i=1}^{N}\|\vec{p}_i-\vec{q}_i'\|_2$ 3) Calculate translation T_c and rotation R_c using the ICP method. 4) Update $P=R_c\cdot P+T_c$, $T=R_c\cdot T+T_c$, $R=R_c\cdot R$.
Stop condition	$\bar{E}_{PQ}$ is less than a threshold E_T or the iterative number reaches the maximal number K.

2) Dealing With Trivial Branches: Due to complex features of palmprint, after the postprocessing, some palmprint principal lines can still have some branches which will decrease the convergence speed and accuracy of the ICP algorithm. In contrast, plain and clear principal line features will make the ICP algorithm converge correctly and rapidly. Here, we propose to use the following three steps to remove small branches.

Step 1: Find all the lines which have no branches using a line tracking method. This step will break the line at all intersections, as shown in Fig. 6(b).

Step 2: Connect the branches which have the same or nearly the same direction at intersections, as shown in Fig. 6(c). Note that the directions of lines have already been calculated by (3) in the previous steps.

Step 3: Remove the branches which are shorter than the half length of the longest branch connected by step 2, as shown in Fig. 6(d).

3) Dealing With Poor-Quality Principal Lines: With the proposed line extraction procedures, the principal lines of most palmprint samples can be well extracted, yet there are still some samples which are hard to extract stable principal lines. Fig. 7 shows some examples. These unstable principal lines can lead to incorrect alignment by using the ICP method. Fortunately, it is very easy to judge if the ICP-based alignment is correct or not based on the mean distance of the corresponding point pairs $\bar{E}_{PQ}$ (see Table I) of the two samples. After ICP alignment, if $\bar{E}_{PQ}$ is less than a preset threshold E_T, we think that the ICP alignment is correct and accept it for the following matching process. Otherwise, we keep the original ROI and ignore the ICP alignment.

III. ALIGNMENT REFINEMENT FOR PALMPRINT RECOGNITION

Once the principal lines are extracted, they can be used for palmprint alignment refinement by using the ICP algorithm. In this section, we first present the principal line-based ICP alignment algorithm to correct the translation and rotation between the ROI images and, then, present an efficient way to incorporate the alignment result into the competitive coding method for palmprint recognition.

A. Principal Line-Based Iterative Closest Point Alignment

ICP algorithm was first proposed by Besl and McKay [14] for registration of 3-D shapes. The key step of ICP algorithm is to estimate the translation parameters *T*, rotation parameter *R*, and scaling parameter *S* between two point sets by minimizing the distance between correspondence points. In palmprint recognition, there is little scaling variation in the palmprint sample images because the distance between the palm and the camera is fixed [3]. Therefore, we ignore the scaling factor *S* in the following development. This can also improve the speed of ICP process.

We adopt the classical ICP method to estimate the transformation parameters between two palmprint images according to their principal lines and, then, use the estimated *T* and *R* to correct the possible translation and rotation variations between them. Fig. 8 illustrates the proposed alignment process. The principal lines are first extracted from the two original ROI images using the method described in Section II, and then, the parameters *T* and *R* are estimated by applying ICP to the extracted principal lines. Finally, one ROI image can be corrected by *T* and *R* to match with another one.

The pseudocode of the aforementioned principal line-based ICP alignment refinement algorithm of palmprint ROI images is summarized in Table I.

B. Feature Extraction and Matching

The CompCode [4] is an effective algorithm for palmprint feature extraction and recognition. It estimates the direction of each point of a palmprint image by six Gabor filters with different orientations and, then, codes the estimated directions

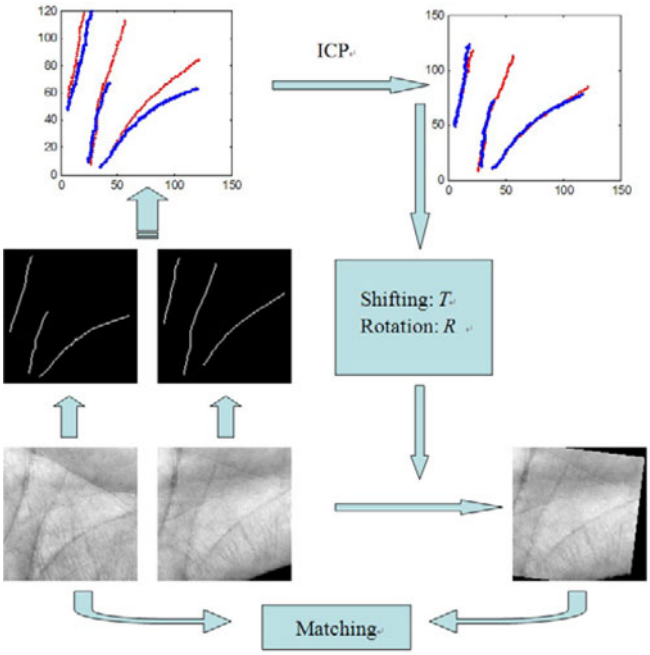

Fig. 8. Principal line-based ICP alignment refinement of two ROIs.

as palmprint features for matching. In this paper, the CompCode is used in joint with the ICP alignment refinement scheme for palmprint recognition. The following Gabor filter is used for directional feature extraction [20]:

$$\psi(x, y, \omega, \theta) = \frac{\omega}{\sqrt{2\pi}\kappa} e^{-(\omega^2/8\kappa^2)(4x'^2+y'^2)}\left(e^{i\omega x'} - e^{-\kappa^2/2}\right) \tag{4}$$

where $x' = (x - x_0)\cos\theta + (y - y_0)\sin\theta$ and $y' = -(x - x_0)\sin\theta + (y - y_0)\cos\theta$; $(x_0,\ y_0)$ is the center of the function, ω is the radial frequency in radians per unit length, θ is the orientation of the Gabor functions in radians, and κ is a coefficient defined by

$$\kappa = \sqrt{2\ln 2}\left(\frac{2^\delta + 1}{2^\delta - 1}\right) \tag{5}$$

where δ is the half-amplitude bandwidth of the frequency response.

In general, it is enough to use six orientations in the Gabor-filter-based directional feature extraction. Using more orientations cannot improve much the accuracy but increase the computational cost. Therefore, we employ six orientations in the directional feature extraction and set $\theta \in \Theta = \{0, \pi/6, 2\pi/6, 3\pi/6, 4\pi/6, 5\pi/6\}$. After convolving the palmprint image with the six Gabor filters of different orientations, at each position, the orientation which leads to the greatest response is selected as the directional feature at that position:

$$D(x, y) = \arg\max_{\theta\in\Theta}\left(\psi(x, y, \omega, \theta) * H\right) \tag{6}$$

where H represents the input palmprint ROI image. Fig. 9 shows two examples of directional feature map $D(x, y)$ of two ROI images.

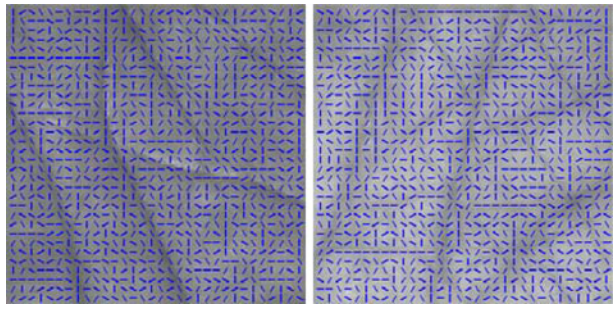

Fig. 9. Examples of directional feature maps.

TABLE II
EER, FEATURE EXTRACTION TIME, AND AVERAGE MATCHING TIME BY DIFFERENT METHODS ON POLYU DATABASE

Methods	EER	Feature extraction time	Matching time
Proposed ICP+CompCode	0.0201%	255ms	0.62ms
CompCode [4]	0.0388%	97ms	0.11ms
Proposed ICP+RLOC	0.0571%	191ms	3.14 ms
RLOC [13]	0.0653%	23ms	0.17ms
Proposed ICP+OrdCode	0.0633%	366ms	1.89ms
OrdCode [6]	0.0878%	61ms	0.20ms

For verification (i.e., 1:1 matching) application, after computing the parameters T and R by the ICP algorithm, we can apply the correction to one of the two ROI images. Then, the Gabor-filtering-based directional feature extraction, coding, and matching procedures can be performed for recognition. The whole verification time is less than 0.5 s, which is fast enough for real-time applications (see Table II for more information about the running time). However, for identification (i.e., 1:N matching) application, correcting ROI images with the estimated T and R parameters and then performing feature extraction again is not a good strategy because Gabor-filtering-based directional feature extraction spends much longer time than matching (see Table II). Actually, in identification, we only need to do feature extraction once for each template sample. We can correct the orientation feature map directly, instead of correcting the image first and then extracting features from the corrected image.

For each point in the feature map extracted by the aforementioned Gabor filters, we denote by θ the orientation, and by (x, y) the location. Let $R = \begin{bmatrix} \cos\theta_R & -\sin\theta_R \\ \sin\theta_R & \cos\theta_R \end{bmatrix}$ be the rotation matrix and $T = [t_x \ \ t_y]$ be the translation vector computed by ICP. The corrected orientation $\theta\prime$ and location (x', y') are calculated as follows:

$$\theta' = \theta + \theta_R \tag{7}$$

$$\begin{bmatrix} x' \\ y' \end{bmatrix} = R \cdot \begin{bmatrix} x \\ y \end{bmatrix} + T. \tag{8}$$

The corrected direction θ' is quantized into one of the six orientations $\{0,\ \pi/6,\ 2\pi/6,\ 3\pi/6,\ 4\pi/6,\ 5\pi/6\}$, and then, we code them with integer values 0, 1, 2, 3, 4, and 5, respectively. We intuitively define the distance between parallel directions as 0, the distance between perpendicular directions as 3, the distance as 1 when the angle of the two directions is $\pi/6$ or $5\pi/6$, and the distance as 2 when the angle of the two directions is

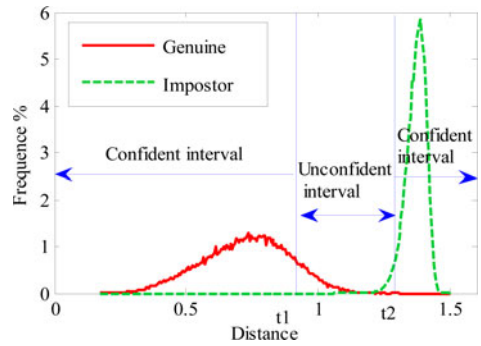

Fig. 10. Confident and unconfident intervals of a typical palmprint matching score distribution.

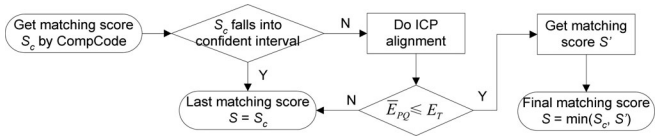

Fig. 11. Flowchart of the proposed matching strategy.

$2\pi/6$ or $4\pi/6$. Let D_d and D_t be the two coded feature maps of two palmprint ROI images; the matching score between them can be defined as

$$S_D = \frac{\sum_{i=1}^{n}\sum_{j=1}^{m} F\left(D_d(i,j), D_t(i,j)\right)}{nm} \tag{9}$$

where

$$F(\alpha,\beta) = \min\left(|\alpha-\beta|,\ 6-|\alpha-\beta|\right),$$
$$\alpha,\beta \in \{0,1,2,3,4,5\}. \tag{10}$$

Here, $F(\alpha,\beta)$ represents the angle distance between α and β whose value can be 0, 1, 2, or 3 as described previously. Finally, if the distance S_D is less than a threshold, the two palmprint images are recognized to be from the same person.

To further improve the efficiency of the whole palmprint recognition system, we do the above ICP alignment when it is really necessary. By using the CompCode method [4], we show a classical matching score distribution of palmprint verification in Fig. 10. We can divide the score axis into two parts: one is the confident interval which is outside of two threshold t_1 and t_2, and the other is the unconfident interval which is between t_1 and t_2, as illustrated in Fig. 10. From Fig. 10, we can see that if the matching score S_c falls into the confident interval, we can easily and correctly decide whether the test sample is a genuine or an imposter. Then, we can accept this score as the last matching score. Otherwise, we do the proposed alignment. And then, if the mean distance of the corresponding point pairs $\bar{E}_{PQ}$ of the two samples is greater than a given threshold E_T, we accept S_c as the final matching score. Otherwise, we match them again by (9) to get a new matching score S'. Then, min(S_c, S') is regarded as the final matching score. This can avoid the incorrect alignment by the ICP method. The flowchart of the used matching strategy is shown in Fig. 11.

IV. Experimental Results

We test the proposed principal line and ICP-based palmprint alignment and recognition method on both the Hong Kong Polytechnic University (PolyU) open palmprint database [21] and the Chinese Academy of Sciences' Institute of Automation (CASIA) open palmprint database [23]. The PolyU database contains 7752 samples collected from 386 different palms in two sessions. The CASIA database contains 5502 palmprint images captured from 312 subjects. An ROI is extracted from the original palmprint image using the method in [3] and [24] for PolyU and CASIA database separately. We then extract the principal lines and perform the ICP alignment, feature extraction, and matching on those ROI images.

To evaluate the verification accuracy of the proposed method, each palmprint image is matched with all the other palmprint images in the database. A successful matching is called intraclass matching or genuine if the two samples are from the same palm. Otherwise, the unsuccessful matching is called interclass matching or impostor. The total number of matchings is 30 042 876. The experiments were performed on a PC with Core 2 CPU @ 2.66 GHz with 2-GB RAM.

A. Comparison With Representative Algorithms

On PolyU database, the proposed principal line and ICP-based palmprint alignment scheme is used in joint with three state-of-the-art palmprint recognition algorithms: CompCode [4], RLOC [13], and OrdCode [6], respectively. CompCode, RLOC, and OrdCode represent the best palmprint recognition techniques, and they achieve the highest accuracy among the existing algorithms. Fig. 12 plots the receiver operator characteristic (ROC) curves of the proposed methods in comparison with the original methods. Table II lists the equal error rate (EER), feature extraction time, and average matching time of the aforementioned methods. For the proposed methods, the feature extraction process includes ROI extraction, principal line extraction, orientation feature extraction, and coding, while the matching process includes ICP alignment refinement and feature map matching. The longest ICP alignment time for two matching samples in our method is about 1.5 ms.[1] Of course, the number of the principal line points also affects the complexity of the ICP algorithm. However, after the process of principal line extraction, the maximum number of the principal line points is less than 600. Most of them have only about 200–400 points, and because of the simple structure of principal lines, the ICP algorithm can converge very fast. Therefore, the ICP algorithm is fast enough for real-time implementation. From Fig. 12 and Table II, we can see that the proposed methods have much higher accuracy than their original counterparts. Especially, the proposed ICP + CompCode method achieves about 48.2% improvement over the original CompCode method, and it has the highest accuracy in all the schemes. Although the speed of feature extraction and matching of the proposed methods is slower than the original methods because of the additional cost of ICP

[1]The longest ICP alignment time is obtained when the ICP algorithm stops at the maximal iteration number, which is set as 10 in our

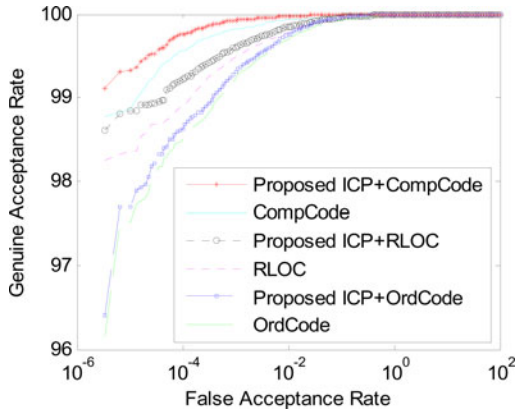

Fig. 12. ROC curves by different methods on PolyU database.

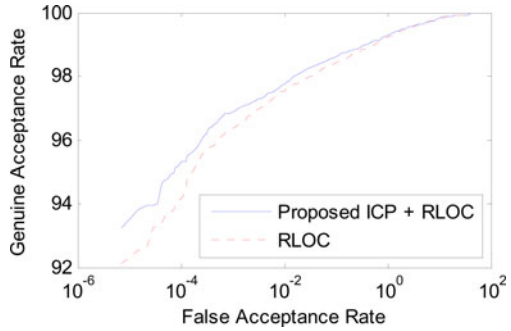

Fig. 13. ROC curves by different methods on CASIA database.

TABLE III
EER, FEATURE EXTRACTION TIME, AND AVERAGE MATCHING TIME BY DIFFERENT METHODS ON CASIA DATABASE

Methods	EER	Feature extraction time	Matching time
Proposed ICP+RLOC	0.794 %	191ms	3.14 ms
RLOC [13]	0.814 %	23ms	0.17ms

alignment, it is still fast enough for real-time implementation. For identification, the feature extraction of the template samples in the database can be done offline. For a test probe image, the feature extraction costs only 255 ms by the proposed method. Meanwhile, the average time per matching by the proposed method is only 0.62 ms. Therefore, for a middle size database with for example 1000 template images, the identification can be finished in 1 s.

On CASIA database, the proposed principal line and ICP-based palmprint alignment scheme is used in joint with RLOC method. Fig. 13 plots the ROC curves of the proposed methods in comparison with the original methods. Table III lists the EER, feature extraction time, and average matching time. We can see that the proposed method also improves the accuracy greatly on CASIA database.

B. Comparison With Template-Shifting-Based Matching Method on the Hong Kong Polytechnic University Database

Shifting the template for matching is also an approach to reducing the misalignment. Therefore, it is necessary to compare the proposed method with the template-shifting-based matching method. The shifting contains translation shifting and rotation shifting. According to our experience, in the experiments, a range between –4 and 4 pixels was used for translation shifting, and a range between –6° and +6° was used for rotation shifting. The step size of translation shifting is 1 pixel. Therefore, there are $9 \times 9 = 81$ cases for translating the template up, down, left, and right. For rotation shifting, the step size is set as 0.5°, 1°, 2°, 3°, and 4°, respectively, in our experiments, and there are 25, 13, 7, 5, and 4 cases for each step size to rotate the template. Therefore, combining the translation shifting with the rotation shifting, there are 2025, 1053, 567, 405, and 324 different matchings with rotation step size being 0.5°, 1°, 2°, 3°, and 4°, respectively. We can see that although the once template matching is very fast, the total template-shifting-based matching process can still be time consuming compared with the proposed ICP alignment method.

To save the matching time, we also adopt the matching strategy illustrated in Fig. 11 for the template-shifting-based matching experiments. If the CompCode matching score falls into the confident interval, then we accept this matching score as the final score instead of doing the template shifting and matching; otherwise, we do the template-shifting-based matching and select the minimal matching score as the final score. Fig. 14 plots the ROC curves of template-shifting-based matching and the proposed ICP-based method. Table IV lists the EER, feature extraction time, and average matching time of the two methods. From Table IV, we can see that the lowest EER by template-shifting-based method is 0.0339%, which is much worse than the proposed method. In addition, the proposed method is more efficient than the template-shifting-based method. From the ROC curves in Fig. 14, we can see that although the template-shifting-based method can decrease the EER compared with the CompCode method, it will have worse performance when the false accept rate is very low. The reason can be found from Fig. 15, where the matching score distributions of the proposed method and the template-shifting-based method are plotted. From Fig. 15(b), we can see that by using the template-shifting-based method, although the genuine matching score can be greatly reduced, the imposter matching score will also be greatly reduced. Therefore, blindly shifting the template for matching is not an effective solution to correct the inaccurate alignment in palmprint recognition. On the contrary, the proposed ICP-based method can achieve much better performance because it exploits the texture feature and line feature in palmprint alignment refinement and matching.

C. Identification Experiments

Finally, we conduct identification experiments to test the proposed method. In identification, we do not know the class of the input palmprint but want to identify which class it belongs to. In the experiments, we let the first sample of each class in the database be template and use the other samples as probes. Therefore, there are 7366 probes and 386 templates. The probes were matched with all the templates models, and for each probe, the matching results were ordered according to the matching scores. The rank-one recognition rates are listed in Table V. We see that

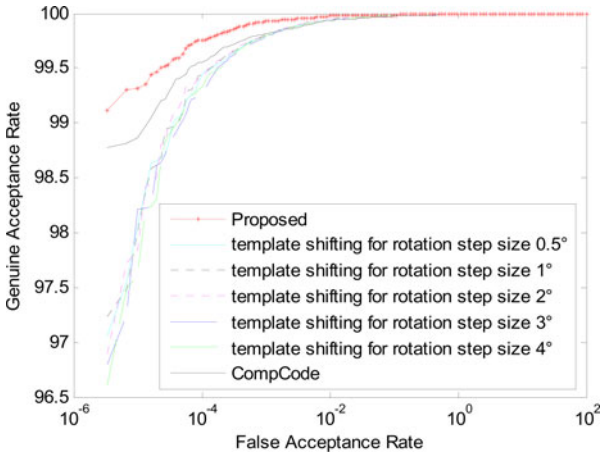

Fig. 14. ROC curves of template-shifting based method and the proposed method.

TABLE IV
EER, FEATURE EXTRACTION TIME, AND AVERAGE MATCHING TIME BY THE TEMPLATE SHIFTING-BASED METHOD AND THE PROPOSED METHOD

Methods		EER	Feature extraction time	Average matching time
Proposed		0.0201%	255ms	0.62ms
CompCode		0.0388%	97ms	0.11ms
Template-shifting based method	Rotation step size 0.5°	0.0353%	153ms	8.17 ms
	Rotation step size 1°	0.0353%	153ms	4.32ms
	Rotation step size 2°	0.0339%	153ms	2.39ms
	Rotation step size 3°	0.0360%	153ms	1.75ms
	Rotation step size 4°	0.0346%	153ms	1.34ms

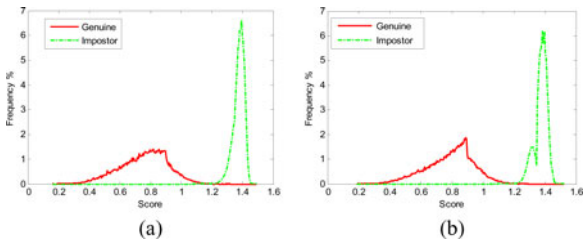

Fig. 15. Matching score distributions by proposed method and the template-shifting based method. (a) By proposed method. (b) By template shifting-based method.

TABLE V
RANK-ONE RECOGNITION RATES BY DIFFERENT METHODS

Method	Proposed ICP+CompCode	CompCode	Proposed ICP+ROC	ROC	Proposed ICP+OrdCode	OrdCode
Rank-one rate	100%	99.98%	100%	99.98%	100%	99.97%

the proposed methods correctly identify all the palmprint images, leading to an identification accuracy of 100%.

V. CONCLUSION

We have proposed a novel alignment refinement strategy for palmprint recognition by applying the ICP method to palmprint principal lines. For the two palmprint images to be aligned, the principal lines were first extracted, and then, the ICP algorithm was used to align the two line datasets. The proposed method can effectively reduce the translation and rotation variations in palmprint images, which are inevitably introduced in the palmprint data acquisition process. In couple with some existing palmprint feature extraction and matching methods, such as CompCode, RLOC, and OrdCode, the proposed method can achieve much higher palmprint recognition accuracy. The experimental results on the HK-PolyU database showed that it could achieve 48.2% improvement over the state-of-the-art CompCode algorithm, leading to the lowest EER of 0.0201%. The proposed method is very powerful for correcting the rotation variations in palmprint images, which is one of the hardest problems to other algorithms. Finally, the proposed method is very fast, and it can be implemented in real time for verification, as well as identification of middle size database.

REFERENCES

[1] W. Shu and D Zhang, "Automated personal identification by palmprint," *Opt. Eng.*, vol. 37, no. 8, pp. 2359–2362, 1998.
[2] T. Cook, R. Sutton, and K. Buckley, "Automated flexion crease identification using internal image seams," *Pattern Recognit.*, vol. 43, pp. 630–635, 2010.
[3] D. Zhang, A. W. K. Kong, J. You, and M. Wong, "On-line palmprint identification," *IEEE Trans. Pattern Anal. Mach. Intell.*, vol. 25, no. 9, pp. 1041–1050, Sep. 2003.
[4] A. W. K. Kong and D. Zhang, "Competitive coding scheme for palmprint verification," in *Proc. Int. Conf. Pattern Recognit.*, 2004, vol. 1, pp. 520–523.
[5] A. K. Jain and J. J. Feng, "Latent palmprint matching," *IEEE Trans. Pattern Anal. Mach. Intell.*, vol. 31, no. 6, pp. 1032–1047, Jun. 2009.
[6] Z. N. Sun, T. N. Tan, Y. H. Wang, and S. Z. Li, "Ordinal palmprint representation for personal identification," in *Proc. IEEE Int. Conf. Comput. Vision Pattern Recognit.*, Jun., 2005, pp. 279–284.
[7] T. Connie, A. T. B. Jin, M. G. K. Ong, and D. N. C. Ling, "An automated palmprint recognition system," *Image Vision Comput.*, vol. 23, no. 5, pp. 501–515, 2005.
[8] A. Kong, D. Zhang, and M. Kamel, "Palmprint identification using feature-level fusion," *Pattern Recognit.*, vol. 39, no. 3, pp. 478–487, 2006.
[9] X. Q. Wu, D. Zhang, and K. Q. Wang, "Palm line extraction and matching for personal authentication," *IEEE Trans. Syst., Man, Cybern. A, Syst., Humans*, vol. 36, no. 5, pp. 978–987, Sep. 2006.
[10] P. J. Shang and T. Li, "Multifractal characteristics of palmprint and its extracted algorithm," *Appl. Math. Modelling*, vol. 33, no. 12, pp. 4378–4387, 2009.
[11] G. K. Michael, T. Connie, and A. B. J. Teoh, "Touch-less palm print biometrics: Novel design and implementation," *Image Vision Comput.*, vol. 26, no. 12, pp. 1551–1560, Dec. 2008.
[12] D. S. Huang, W. Jia, and D. Zhang, "Palmprint verification based on principal lines," *Pattern Recognit.*, vol. 41, no. 4, pp. 1316–1328, Apr. 2008.
[13] W. Jia, D. S. Huang, and D. Zhang, "Palmprint verification based on robust line orientation code," *Pattern Recognit.*, vol. 41, no. 5, pp. 1504–1513, May 2008.
[14] P. J. Besl and N. D. McKay, "A method for registration of 3-D shapes," *IEEE Trans. Pattern Anal. Mach. Intell.*, vol. 14, no. 2, pp. 239–256, Feb. 1992.
[15] K. O. Goh, C. Tee, B. J. Teoh, and C. L. Ngo, "Automated hand geometry verification system based on salient points," in *Proc. 3rd Int. Symp. Commun. Inf. Technol.*, 2003, pp. 720–724.
[16] J. Canny, "A computational approach to edge detection," *IEEE Trans. Pattern Anal. Mach. Intell.*, vol. 8, no. 6, pp. 679–698, Nov. 1986.

[17] R. O. Duda, P. E. Hart, and D. G. Stork, *Pattern Classification*, 2nd ed. New York: Wiley-Interscience, 2000.
[18] J. Radon, "Über die bestimmung von funktionen durch ihre integralwerte längs gewisser mannigfaltigkeiten," *Berichte Sächsische Akademie der Wissenschafter*, vol. 69, pp. 262–267, 1917.
[19] K. S. Arun, T. S. Huang, and S. D. Blostein, "Least-squares fitting of two 3-D point sets," *IEEE Trans. Pattern Anal. Mach. Intell.*, vol. 9, no. 5, pp. 698–700, Sep. 1987.
[20] T. S. Lee, "Image representation using 2D Gabor wavelet," *IEEE Trans. Pattern Anal. Mach. Intell.*, vol. 18, no. 10, pp. 959–971, Oct. 1996.
[21] PolyU Palmprint Database, Biometric Research Centre, The Hong Kong Polytechnic University. (2003). [Online]. Available at http://www.comp.polyu.edu.hk/∼biometrics/
[22] W. Li, L. Zhang, D. Zhang, and J. Q. Yan, "Principal line based ICP alignment for palmprint verification," in *Proc. IEEE Int. Conf. Image Process.*, Nov., 2009, pp. 1961–1964.
[23] CASIA Palmprint Database. (2005). [Online]. Available: http://biometrics.idealtest.org/
[24] Z. Guo, W. Zuo, L. Zhang, and D. Zhang, "A unified distance measurement for orientation coding in palmprint verification," *Neurocomputing*, vol. 73, no. 4–6, pp. 944–950, Jan. 2010.
[25] Y. Pang, X. Li, Y. Yuan, D. Tao, and J. Pan, "Fast Haar transform based feature extraction for face representation and recognition," *IEEE Trans. Inf. Forensics Security*, vol. 4, no. 3, pp. 441–450, Sep. 2009.
[26] Y. Pang, X. Li, and Y. Yuan, "Robust tensor analysis with L1-norm," *IEEE Trans. Circuits Syst. Video Technol.*, vol. 20, no. 2, pp. 172–178, Feb. 2010.
[27] Y. Pang, Y. Yuan, and X. Li, "Gabor-based region covariance matrices for face recognition," *IEEE Trans. Circuits Syst. Video Technol.*, vol. 18, no. 7, pp. 989–993, Jul. 2008.

Wei Li received the B.S. degree from the Luoyang Institute of Technology, Luoyang, China, in 2001, the M.S. degree in mechanical and electrical engineering from the Henan University of Science and Technology, Luoyang, in 2005, and Ph.D. degree in pattern recognition and intelligent systems from Shanghai Jiao Tong University, Shanghai, China, in 2010.

He is currently an Assistant Researcher with the Shenzhen Institute of Advanced Technology, Chinese Academy of Sciences, Shenzhen, China. His research interests include pattern recognition, image processing, graphics, cloud computing, and virtualization.

Bob Zhang (M'12) received the M.A.Sc. degree from Concordia University, Montreal, QC, Canada, in 2007, and the Ph.D. degree from the University of Waterloo, Waterloo, ON, Canada, in 2011.

He is currently a Researcher with the UW Center for Pattern Analysis and Machine Intelligence in the Department of Electrical and Computer Engineering, University of Waterloo. His research interests include pattern recognition, machine learning, and medical biometrics.

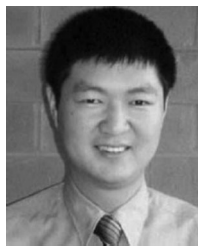

Lei Zhang (M'04) received the B.S. degree from the Shenyang Institute of Aeronautical Engineering, Shenyang, China, in 1995, and the M.S. and Ph.D. degrees in electrical and engineering from Northwestern Polytechnical University, Xi'an, China, in 1998 and 2001, respectively.

From 2001 to 2002, he was a Research Associate with the Department of Computing, The Hong Kong Polytechnic University, Kowloon, Hong Kong, where he has been an Assistant Professor since January 2006. From January 2003 to January 2006, he was a Postdoctoral Fellow with the Department of Electrical and Computer Engineering, McMaster University, Hamilton, ON, Canada. His current research interests include image and video processing, biometrics, pattern recognition, multisensor data fusion, and optimal estimation theory.

Jingqi Yan received the B.S. degree in automatic control in 1996, and the M.S. and Ph.D. degrees in pattern recognition and intelligent systems in 1999 and 2002, respectively, from Shanghai Jiao Tong University, Shanghai, China.

He is currently a Researcher with the Institute of Image Processing and Pattern Recognition, Shanghai Jiao Tong University. His interests include geometric modeling, computer graphics, biometrics, scientific visualization, and image processing.